Supporting information for

Oxygen vacancies engineering ultra-small $CuWO_4$ nanoparticles for boosting photocatalytic organic pollutant degradation

Dingzhou Xiang, Xin Jin, Guilin Sun, Chenghuan Zhong, Shan Gao*

School of Chemistry and Chemical Engineering, Faculty of materials science and engineering, Anhui Province Key Laboratory of Chemistry for Inorganic/Organic Hybrid Functionalized Materials, Key Laboratory of Structure and Functional Regulation of Hybrid Materials of Ministry of Education, Anhui University, 230601 Hefei, Anhui, P.R. China

*Corresponding author: shangao@ahu.edu.cn.

1. Experimental section

1.1 Materials

Sodium tungstate dihydrate ($Na_2WO_4·2H_2O$, AR, 99.5%), methylene blue (MB) and 5,5-Dimethyl-1-pyrroline N-oxide (DMPO) were purchased from Shanghai Macklin Biochemical Co., Ltd. Sodium oleate (CP) was purchased from Shanghai Aladdin Biochemical Technology Co., Ltd. Copper chloride dihydrate ($CuCl_2·2H_2O$, AR), ammonia solution ($NH_3·H_2O$, AR), hydrochloric acid (HCl, AR) and ethanol absolute (C_2H_6O, AR) were purchased from Shanghai Sinopharm Chemical Reagent Co. Ltd. All the reagents used as received without further purification.

1.2 Catalyst Preparation

***Synthesis of $CuWO_4$-Air*:** Typically, 20 mg CP was dispersed into 30 mL ultrapure water under vigorous stirring for 0.5 h. Whereafter 1.5 mmol $CuCl_2·2H_2O$ was added and kept stirring for 0.5h, and then 1.5 mmol $Na_2WO_4·2H_2O$ was added to the above solution. After stirring for 0.5 h, 0.25 mL $NH_3·H_2O$ was dropwise added, the pH of the solution was adjusted to 8~9 by dropping appropriate HCl aqueous solution (1 M) to form a homogenous suspension, then the mixture was

transferred to the 50 mL of Teflon-lined autoclave and heated at 180 ℃ for 12 h. After cooling to room temperature, the green precipitate was collected by centrifuging and washed with cyclohexane and ethanol several times and then dried in a vacuum-freezing drier for 12 h. The final product was directly calcined at 500 ℃ in the air for 1 h and then naturally cooled to ambient temperature, denoted as $CuWO_4$-Air.

***Synthesis of $CuWO_4$-OVs 350*:** In detail, a small quantity of $CuWO_4$-Air was ground into powder and then evenly spread at the bottom of an alumina combustion boat. The boat containing catalysts was thermally treated in a stream of H_2/Ar (v/v = 5%/95%) mixed gas atmosphere at temperatures of 350 ℃ for 15 min to obtain $CuWO_4$ with abundant oxygen vacancies, labeled as $CuWO_4$-OVs 350.

1.3 Characterizations

The crystal structures of the samples were analyzed by using an X-ray powder diffractometer (XRD, SmatrLab9kW, Japan) equipped with Cu Kα radiation (λ = 0.15418 nm). Transmission electron microscopy (TEM) and high-resolution TEM (HRTEM) images were obtained on a JEM-2100 transmission electron microscope (JEOL). X-ray photoelectron spectra (XPS) was measured using the ESCALAB 250Xi spectrometer with an Al anode (Al Kα = 1846.6 eV). The Raman spectroscopy was performed by a Thermo Scientific Xplora Plus confocal spectrometer with an Olympus BX43 microscope. Fourier transform-infrared (FT-TR) spectroscopy was recorded on a Nicolet iS50 Fourier-transform infrared spectrometer (Thermo Scientific, Warsaw, Poland) using KBr pellet support. The specific surface area was obtained by the Brunauer-Emmett-Teller (BET) method and measured by using a Micromeritics ASAP 2020 at 77 K with N_2 physical adsorption. Electron paramagnetic resonance (EPR) spectroscopy was carried out on a Bruker A300 EPR spectrometer at room temperature. UV-visible spectra were measured using a U-4100 photodiode array spectrophotometer. The photoluminescence spectra were measured in an F-4500 FL Spectrophotometer with an exciting wavelength of 320 nm. Photoelectrochemical tests were performed on the CHI 760E electrochemical workstation.

1.4 Density-functional theory calculations

The QuantumWise Atomistix ToolKit (ATK) 2020 software [1] was used to perform the density-functional theory (DFT) calculations in this paper. Herein, the linear combination of atomic

orbitals (LCAO) basis set was chosen combined with the hybrid Hybrid-Scuseria-Ernzerhof (HSE06) exchange-correlation [2]. The pseudopotential was set as PseudoDojo which was precise enough [3]. The density mesh cut-off was set as 100 Hartree, and the tolerance was 1×10-5 eV for energy and 0.02 eV/Å for force. The initial k-point mesh was sampled by the Monkhorst-Pack method with a separation of 0.04 Å. Then, the separation of 0.02 Å was used for the partial density of states (PDOS) calculations.

1.5 Photocatalytic degradation experiments

To explore the photocatalytic activities of $CuWO_4$ catalysts, all the photodegradation tests were conducted in a homemade quartz container. 20 mg photocatalyst was dispersed in 50 mL MB (10 mg L^{-1}) solution to form uniform suspension under ultrasonication. Then the mixed suspension was magnetically stirred for 30 min in the dark to reach an adsorption-desorption equilibrium. In the photodegradation process, the 300 W Xenon light with a 420 nm cut-off filter was used as the light source. 1.5 mL suspension was pipetted every 10 min, and centrifuged. Finally, the absorbance of the filtrate was detected using a UV-2450 spectrophotometer. The catalyst was collected and reused after a full photocatalytic test. The recycling experiments were carried out five times. The reaction system temperature was maintained stable through a recycled cooling water system.

1.6 Hydroxyl radical trapped experiment

The suspension was prepared according to the photocatalytic degradation experiment. Then 20 μL scavenger agents (DMPO) was added into 4 mL suspension under ultrasonication. Afterwards, the mixed suspension was transfer to nuclear magnetic tube for electron spin resonance (ESR) measurement. The generated $^{\bullet}OH$ radical in photocatalytic process ($\lambda > 420$ nm) was captured by DMPO and then the signal was detected on the electron spin resonance spectrometer (A300-10/12, Bruker).

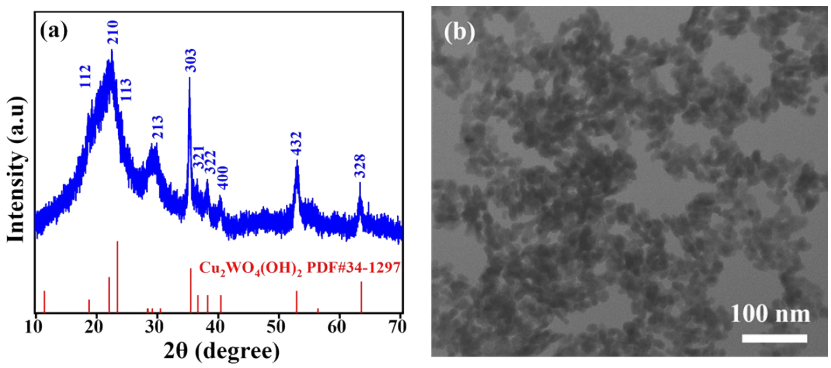

Fig. S1. (a) XRD pattern and (b) TEM image for $Cu_2WO_4(OH)_2$.

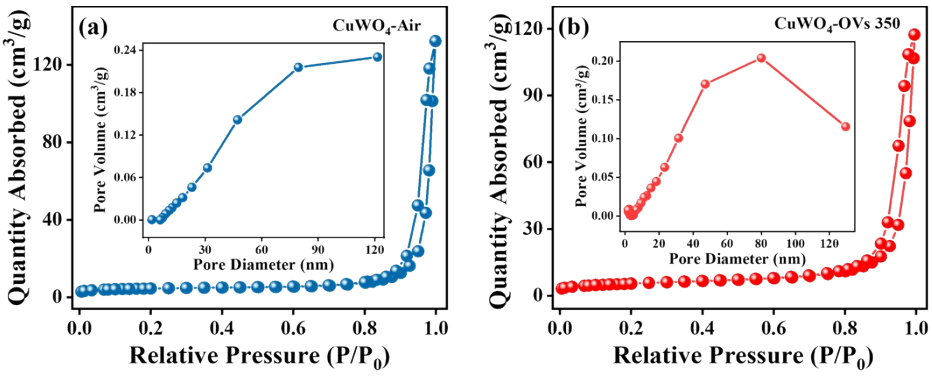

Fig. S2. N_2-isothermal adsorption and desorption curves of (a) $CuWO_4$-Air, (b) $CuWO_4$-OVs 350.

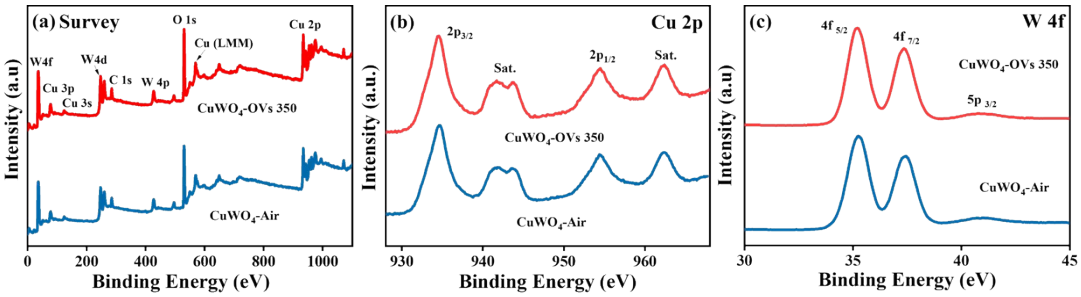

Fig. S3. XPS spectra of (a) Survey, (b) Cu 2p and (c) W 4f for $CuWO_4$-Air and $CuWO_4$-OVs 350.

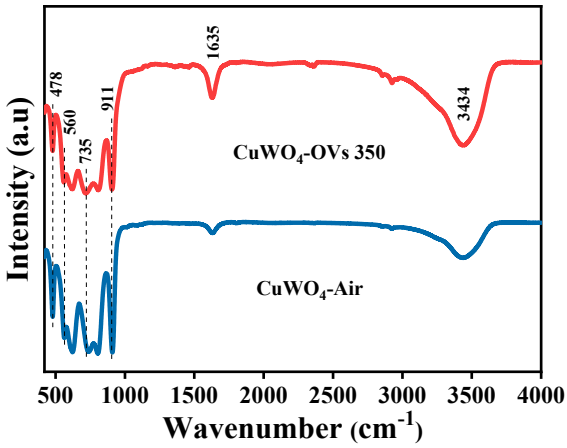

Fig. S4. FT-IR spectra of $CuWO_4$-Air and $CuWO_4$-OVs 350.

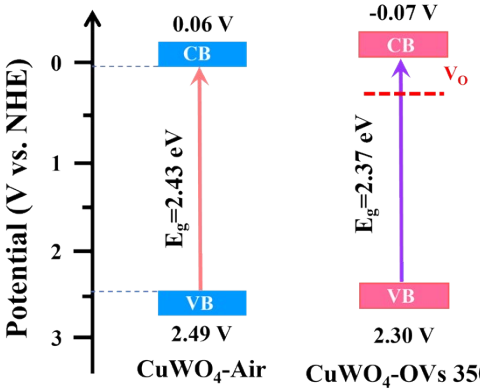

Fig. S5. Schematic illustration of the band structures for $CuWO_4$-Air and $CuWO_4$-OVs 350.

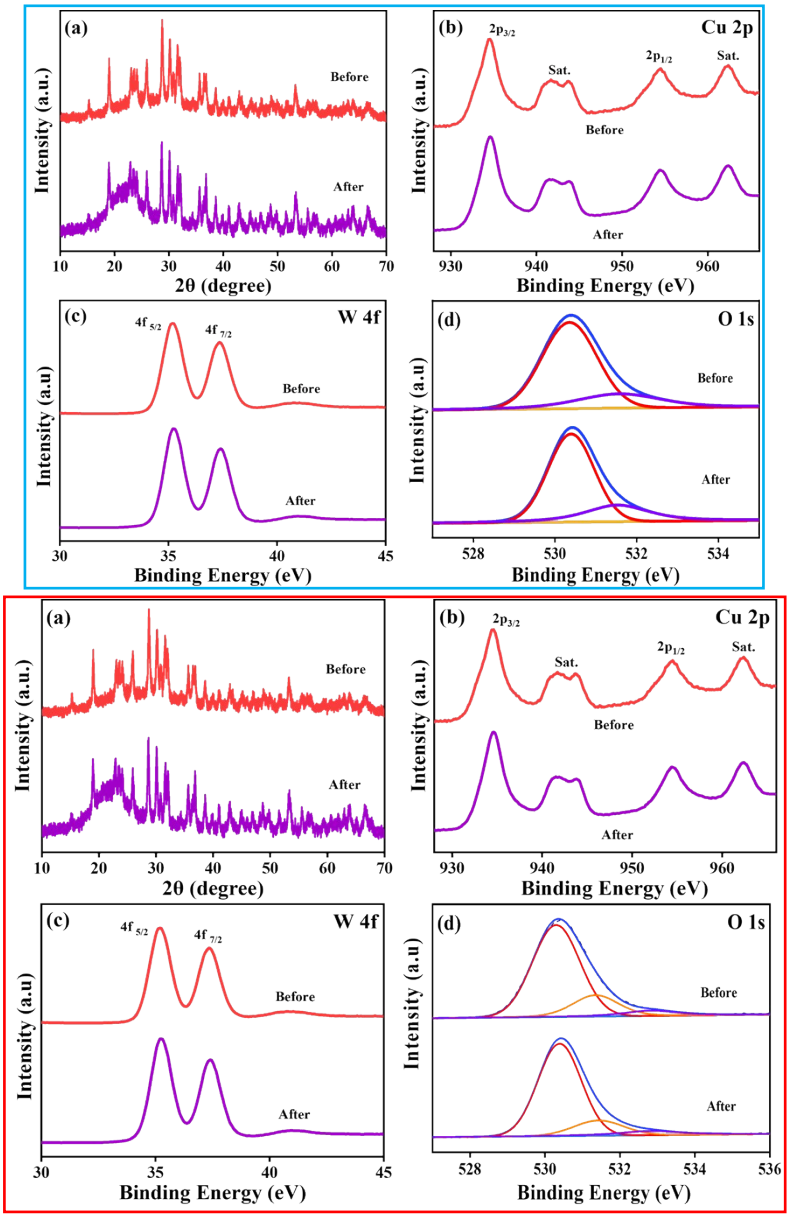

Fig. S6. (a) XRD pattern, (b) Cu 2p, (c) W 4f and (d) O 1s XPS spectra for the fresh and used $CuWO_4$-OVs 350.

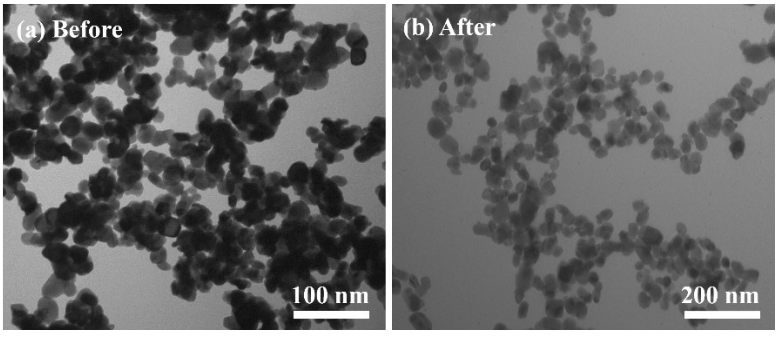

Fig. S7. (a-b) TEM images of the fresh and used $CuWO_4$-OVs 350.

Table S1 BET Surface area (S_{BET}), pore diameter (D_p) and pore volume (V_p) of $CuWO_4$-Air and $CuWO_4$-OVs 350

Samples	S_{BET} ($m^2 \cdot g^{-1}$)[a]	Pore volume ($cm^3 \cdot g^{-1}$)[b]	Average pore size (nm)[b]
$CuWO_4$-Air	19	0.16	53
$CuWO_4$-OVs 350	18	0.17	38

[a] Obtained from BET method.

[b] Total pore volume taken from the N_2 adsorption volume at a relative pressure (P/P_0) of 0.99.

Table S2 Lattice parameters of $CuWO_4$ and $CuWO_4$-OVs unitcell.

	a	*b*	*c*	*α*	*β*	*γ*
$CuWO_4$	9.52 Å	9.86 Å	6.02 Å	87.13°	81.44°	86.31°
$CuWO_4$-OVs	9.63 Å	9.98 Å	6.02 Å	87.29°	81.64°	86.18°

Table S3 Performance comparison of $CuWO_4$-based photocatalysts for Methylene blue degradation.

Photocatalyst	Relevant data	Light source	Pollutants	Removal ratio	Refs
$CuWO_4$-OVs	20 mg of catalyst 50 mL MB aqueous solution (10 mg L^{-1}) S_{BET} = 18 m^2 g^{-1}	300 W Xe lamp ($\lambda \geq 420$ nm)	MB	90.26 % in 70 min	This work
NiAl LDH/$CuWO_4$	100 mg of catalyst 100 mL MB aqueous solution (10 mg L^{-1})	400 W Xe lamp	MB	87.58% in 5 h	[4]
$CuWO_4$@Cu_2O	Catalyst on Cu mesh (2×2 cm^2) 50 mL organic pollutant aqueous solution (0.1 mM)	18 W LED lamp (415 nm $\leq \lambda \leq$ 765 nm)	MB	90.2 % in 120 min	[5]
$CuWO_4$ nanoparticle	30 mg of catalyst 20 mL MB aqueous solution (10 mg L^{-1})	300 W Xe lamp (AM 1.5 G)	MB	70 % in 180 min 99% in 30 min (1 mL H_2O_2)	[6]
Hollow $CuWO_4$	40 mg of catalyst 50 mL MB aqueous solution (20 mg L^{-1}) S_{BET} = 37.11 m^2 g^{-1}	350 W Xe lamp (λ > 420 nm)	MB	95 % in 120 min	[7]

$MOF/CuWO_4$	10 mg of catalyst 50 mL MB aqueous solution 100 mL in capacity S_{BET} = 801 m^2 g^{-1}	5 W LED lamp ($\lambda \geq 420$ nm)	MB	98 % in 135 min	[8]
$CuWO_4/ZnO$	30 mg of catalyst 150 mL MB aqueous solution (20 mg L^{-1}) S_{BET} = 10.88 m^2 g^{-1}	300 W Xe lamp (AM 1.5 G)	MB	98.9 % in 120 min	[9]
Ag-$CuWO_4/WO_3$	40 mg of catalyst 10 mg L^{-1} MB S_{BET} = 56.2 m^2 g^{-1}	200 W Xe lamp ($\lambda \geq 420$ nm)	MB	51% in 180 min	[10]

References:

[1] S. Smidstrup, T. Markussen, P. Vancraeyveld, J. Wellendorff, J. L. Schneider, T. Gunst, B. Verstichel, D. Stradi, P. A Khomyakov, U. G Vej-Hansen, M. E. Lee, S. T Chill, F. Rasmussen, G. Penazzi, F. Corsetti, A. Ojanperä, K. Jensen, M. L N Palsgaard, U. Martinez, A. Blom, M. Brandbyge and K. Stokbro, QuantumATK: An integrated platform of electronic and atomic-scale modelling tools, J. Phys. Condens. Matter, 2019, **32**, 015901.

[2] J. Heyd, G. E. Scuseria and M. Ernzerhof, Hybrid functionals based on a screened Coulomb potential, J. Chem. Phys., 2003, **118**, 8207-8215.

[3] Y. Uemura, A. S. M. Ismail, S. H. Park, S. Kwon, M. Kim, Y. Niwa, H. Wadati, H. Elnaggar, F. Frati, T. Haarman, N. Höppel, N. Huse, Y. Hirata, Y. J. Zhang, K. Yamagami, S.Yamamoto, I. Matsuda, T. Katayama, T. Togashi, S. Owada, M. Yabashi, U. Halisdemir, G. Koster, T. Yokoyama, B. M. Weckhuysen and F. M. F. de Groot, Femtosecond Charge Density Modulations in Photoexcited $CuWO_4$, J. Phys. Chem. C, 2021, **125**, 7329-7336.

[4] S. Megala, A. Silambarasan, S. Kanagesan, M. Selvaraj, P. Maadeswaran, R. Ramesh and M. M. Alam, M. A. Assiri, Interfacial coupling of $CuWO_4$ nanoparticles on NiAl LDH as a novel

photocatalyst for dissolved organic dye degradation, J. Mol. Struct., 2022, **1252**, 132149.

[5] C. L. Zhou, J. Cheng, K. Hou, Z. T. Zhu and Y. F. Zheng, Preparation of $CuWO_4$@Cu_2O film on copper mesh by anodization for oil/water separation and aqueous pollutant degradation, Chem. Eng. J., 2017, **307**, 803-811.

[6] M. Waimbo, G. Anduwan, O. Renagi, S. Badhula, K. Michael, J. P. S. Velusamy and Y. S. Kim, Improved charge separation through H_2O_2 assisted copper tungstate for enhanced photocatalytic efficiency for the degradation of organic dyes under simulated sun light. J. Photochem. Photobiol. B Biol., 2020, **204**, 111781.

[7] J. F. Li, Y. B. Chen, Z. Wang and Z. Q. Liu, Self-templating synthesis of hollow copper tungstate spheres as adsorbents for dye removal, J. Colloid Interface Sci., 2018, **526**, 459-469.

[8] H. Ramezanalizadeh and F. Manteghi, Synthesis of a novel MOF/$CuWO_4$ heterostructure for efficient photocatalytic degradation and removal of water pollutants. J. Clean. Prod., 2018, **172**, 2655-2666.

[9] C. Y. Chen, W. Y. Bi, Z. L. Xia, W. H. Yuan and L. Li. Hydrothermal synthesis of the $CuWO_4$/ZnO composites with enhanced photocatalytic performance, ACS Omega, 2020, **5**, 13185-13195.

[10] R. Salimi, A. A. Sabbagh Alvani, N. Naseri, S. F. Du and D. Poelman, Visible-enhanced photocatalytic performance of $CuWO_4$/WO_3 hetero-structures: Incorporation of plasmonic Ag nanostructures, New J. Chem., 2018, **42**, 11109-11116.